Solid State Science and Technology, Vol. 33, No. 2 (2025) 66-76
https://doi.org/10.66514/ssst3326676x

Effect of Natural Dye Photosensitizer from Mangosteen Pericarp, Purple Grape Peel and Violet Bougainvillea Petal on Solid-State Dye-Sensitized Solar Cell

Hasiah Salleh[1,2,], Ahmad Nazri Dagang[1,2] , Nik Aziz Nik Ali[3], Nur Salihah Alias[1], Nurul Alfatihah Mohd Arifin[1]*

[1]Faculty of Ocean Engineering Technology, Universiti Malaysia Terengganu, 21030 Kuala Nerus, Terengganu, Malaysia

[2]Renewable Energy & Power Research Interest Group, Faculty of Ocean Engineering Technology, Universiti Malaysia Terengganu, 21030 Kuala Nerus, Terengganu, Malaysia

[3]Faculty of Fisheries and Food Science, Universiti Malaysia Terengganu, 21030 Kuala Nerus, Terengganu, Malaysia

**Corresponding author: hasiah@umt.edu.my*

(Received: 28 March 2025 / Revised: 26 June 2025 / Accepted: 1 July 2025 / Published online: 3 July 2025)

ABSTRACT

Hybrid solar cells are a promising potential replacement for inorganic semiconductorbased solar cells. This work focused on solid-state dye-sensitized solar cells fabricated using grown ZnO nanorods and natural dyes extracted from Garcinia mangostana l. pericarp (GMP), Vitis vinifera peel (VVP) and Violet bougainvillea sp. petals (VBP), which were used as a photosensitizer. The zinc oxide nanorod was successfully grown via the hydrothermal method, with an average diameter of ~76.7 nm. The absorption spectra of GMP, VVP and VBP showed a broad absorption spectrum from 400 nm to 700 nm. The GMP exhibited the lowest energy gap (1.82 eV) compared to VVP and VBP. The solid-state dye-sensitized solar cell's zinc oxide nanorod fabricated using natural dye photosensitizers showed that GMP contributed the highest power conversion efficiency of 0.72%.

Keywords: Solid-state dye-sensitized solar cell; zinc oxide nanorod; mangosteen pericarp; Vitis Vinifera peel; Violet Bougainvillea petals

INTRODUCTION

Recently, many efforts have been expended to save the world from pollution and the limited supply of resources. Old energy production was facing serious air pollution and limited resources. The next generation needs to 100% utilize renewable energy. Solar cells can convert visible light into electricity, with a simple operational principle [1]. Various types of solar cells convert sunlight into electricity. Among the various thirdgeneration solar cells, solid-state dye-sensitized solar cells (SS-DSSC) can still be developed in the research process to increase their efficiency comparable to the efficiency of silicon solar cells. Improving the efficiency of SS-DSSC depends on a long, hard and careful process; the well-being of the environment should not be neglected. Therefore, natural dye is used to fabricate SS-DSSC with metal oxide, zinc oxide.

The addition of natural pigments as sensitizing dyes in solar cell fabrication has recently attracted increasing attention in solar cell technology, as opposed to synthetic ones[2]. Synthetic dyes commonly used in the solar industry are suspected of polluting the environment via their waste and being unfriendly compared to dyes extracted from natural resources [3]. Another issue was that synthetic dyes seem undesirable due to their high cost and complex synthesis processes [4]. One of the natural pigments used as a sensitizer is anthocyanin. Anthocyanins are natural components that mostly give redpurple colouration to fruits, plants and flowers [5]. Anthocyanin pigments are dyes with high potential as sensitizers due to their ability to absorb light at the longest wavelength in the 520-550 nm [6].

Although titania is the most commonly used metal oxide in dye-sensitized solar cells, some researchers have sought to employ zinc oxide (ZnO) due to its inexpensive cost, faster electron mobility and a higher energy level in the conduction band, resulting in better electron injection. ZnO was the first material employed in experimental design to prove the irreversible electron injection of organic molecules into the conduction band of metal oxide [7]. The structure of ZnO was in various shapes and sizes. Recent research has been more focused on rods and nano-sized materials. So, when ZnO nanorods were combined with natural dye, the surface area of dye absorption was increased.

The objective of this paper was to investigate the potential of natural dye contained in the purple colour of the plant parts, which were *Garcinia mangostana L*. pericarp, *Vitis vinifera* peels and *Violet bougainvillea Sp*. petals as photosensitizers in SS-DSSCs. In this work, natural dyes extracted from *Garcinia mangostana L*. pericarps, *Vitis vinifera* peels and *Violet bougainvillea Sp*. petals. The dominant pigment extracted from these three plants is anthocyanin. The SS-DSSCs fabricated started with ZnO nanorods grown by the hydrothermal method. The ZnO nanorods are immersed in natural dye solution. The optical and electrical properties of natural dyes were studied as photosensitisers, followed by an investigation of solar behaviour in SS-DSSCs.

MATERIALS AND METHODS

Materials

The raw materials for anthocyanin dyes are extracted from the pericarp of *Garcinia Mangostana L.* (GMP), the peels of *Vitis Vinifera* (VVP) and the violet petals of *Bougainvillea Sp.* (VBP). Fresh GMP, VVP and VBP were cut into small pieces to enable

faster drying. Then, the sliced materials were washed several times with distilled water to remove dirt and oven dried at 59 ºC for 12 h. Sofyan *et al.* have recently developed a methodology for increasing the solubility of the raw materials in solvents and enhanced the pigment extraction by grinding the raw materials into powder [2]. The powder was mixed with ethanol at a ratio of 1: 10. Then the solutions were stored in a refrigerator for 3 days. Lastly, the solutions were extracted with filter paper and collected in a beaker. Figure 1 shows the colour of the natural dye solution of the extraction from GMP, VVP and VBP [8, 9].

Preparations of ITO Substrate

Indium-doped tin oxide glasses (ITO) with a size of 1 cm × 2 cm were chosen as transparent conductive oxide substrates for the base of the photoanode. Its conductivity is 0.1 S/cm supplied by the Merck company. There were a few steps for cleaning the ITO by using detergent, distilled water and acetone. The cleaning process used an ultrasonic bath as done by Aziz et al. (2014) [7]. ITO glass was etched at 0.25 cm at the edge of a rectangular shape as shown in Figure 2.

Growth of ZnO nanorods

A simple sol-gel technique was used to make a seed solution for zinc oxide [6]. The grown zinc oxide nanorods were produced using the hydrothermal method. The ITO substrates with zinc oxide seed layers were immersed in a solution of a mixture of 0.04 M hexamethylenetetramine, 20 mL of distilled water and 0.04 M zinc nitrate hexahydrate at 95 ºC for 10 min. Then, the grown zinc oxide film was washed with distilled water several times and dried with a hair dryer [10].

Fabrication of SS-DSSCs

The grown zinc oxide film was then directly immersed in a dye solution for six hours in dark conditions. The synthesized grown zinc oxide was rinsed several times with ethanol to remove unabsorbed dye [5]. On another occasion, poly (3-hexylthiophene) (P3HT) solution was coated on the surface of the zinc oxide nanorods at 1200 rpm for 30 s. Heated at 120 ºC for 10 min on the hotplate to remove solvent. Finally, aluminum was deposited using physical vapor deposition. A complete solid-state dye-sensitized solar cell is shown in Figure 3.

Characterisations of samples

UV-vis spectroscopy was used to characterize the optical absorption properties of natural dyes. The UV-Vis absorption spectra of the natural dyes were recorded after dilution in ethanol using a Perkin Elmer Lambda 35 UV-visible spectrophotometer in the wavelength range of 200 to 900 nm [5]. The morphology of the grown ZnO nanorods was viewed via a scanning electron microscope (SEM, JEOUL JSM-6360 LA) to proof the formation of nanorod shape. Two probes with SMU 4200 Keithley measured the power conversion efficiency of the solid-state dye-sensitized solar cell.

Figure 1. Natural purple dyes extracted from (a) mangosteen pericarp, (b) black grape peels and (c) violet Bougainvillea flower. (d–f) The powdery sample was obtained after the drying process. (g–i) The extracted solution of the natural purple dyes

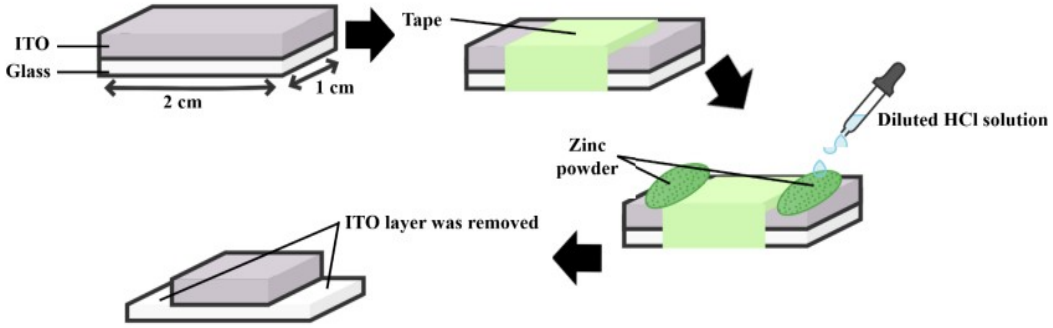

Figure 2. The etching process of ITO glass substrate

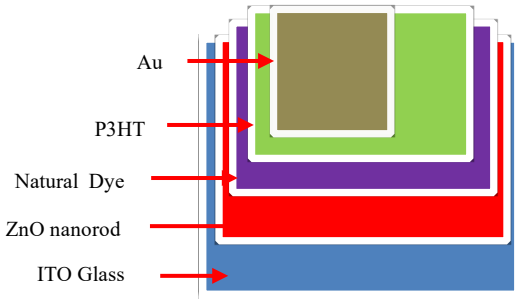

Figure 3. Layer-by-layer of ZnO nanorod, natural dye, P3HT and gold (Au)

RESULTS AND DISCUSSION

Morphology analysis on Zinc Oxide nanorod

Zinc oxide nanorods were grown via the hydrothermal method and baked at 95 ^{o}C for 15 min to form the nanostructure with a thin film thickness as shown in Figure 4. SEM images show that the morphology of grown ZnO deposited on an ITO glass substrate is nanorod-shaped and oriented in a non-specific direction [11], with small hexagonal. The average length and diameter of the nanorods are 237 and 76.7 nm, respectively. The outcome indicates that the ZnO has good crystallinity. It is considered a successful result because the particle size of ZnO is 76.7 nm, which is less than 100 nm [12]. Furthermore, it raised the surface area for the dye attached, facilitating more light to be captured. More electrons move through the cell, increasing the efficiency of the SS-DSSC [13].

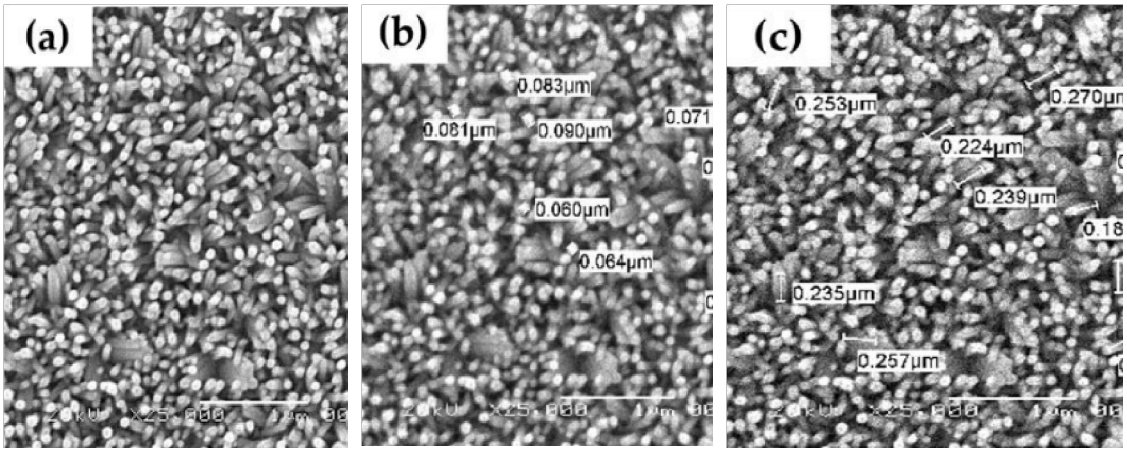

Figure 4. The SEM images of (a) grown ZnO on the ITO glass, (b) diameter of grown ZnO nanorods and (c) length of grown ZnO nanorods measurement

Optical Absorption of GMP GMP, VVP and VBP in solution

Figure 5 shows the UV-visible absorption spectra of the natural dyes used in this study. Figure 5(a) shows that the *garcinia mangostana l.* pericarp (GMP) absorbs in two ranges of light wavelengths, at 400−600 nm and 650−670 nm, with maximum peaks at 401 nm and 665 nm, which are associated with chlorophyll *a*. The broad peaks at wavelength 441 nm and 608 nm are associated with chlorophyll *b*. Another broad peak at wavelength 540 nm is associated with anthocyanin. Meaning that an extensive range of light spectrum was absorbed by pigments in the GMP [14]. Extraction of *vitis vinifera* peel, VVP of fruit (VVP) (Figure 5(b)) shows the presence of anthocyanin with a broad absorption from 470−550 nm [3]. Meanwhile, Figure 5(c) shows the absorption spectrum of *violet bougainvillea* petal (VBP) extract with two absorption peaks found at 409 nm and 665 nm, which can be associated with chlorophyll *a*. And there was the presence of chlorophyll *b* appeared at the broad peak of 441 nm and 608 nm. The anthocyanin pigment absorbance is estimated from 450 to 570 nm with two broad peaks at 469 nm and 535 nm [15].

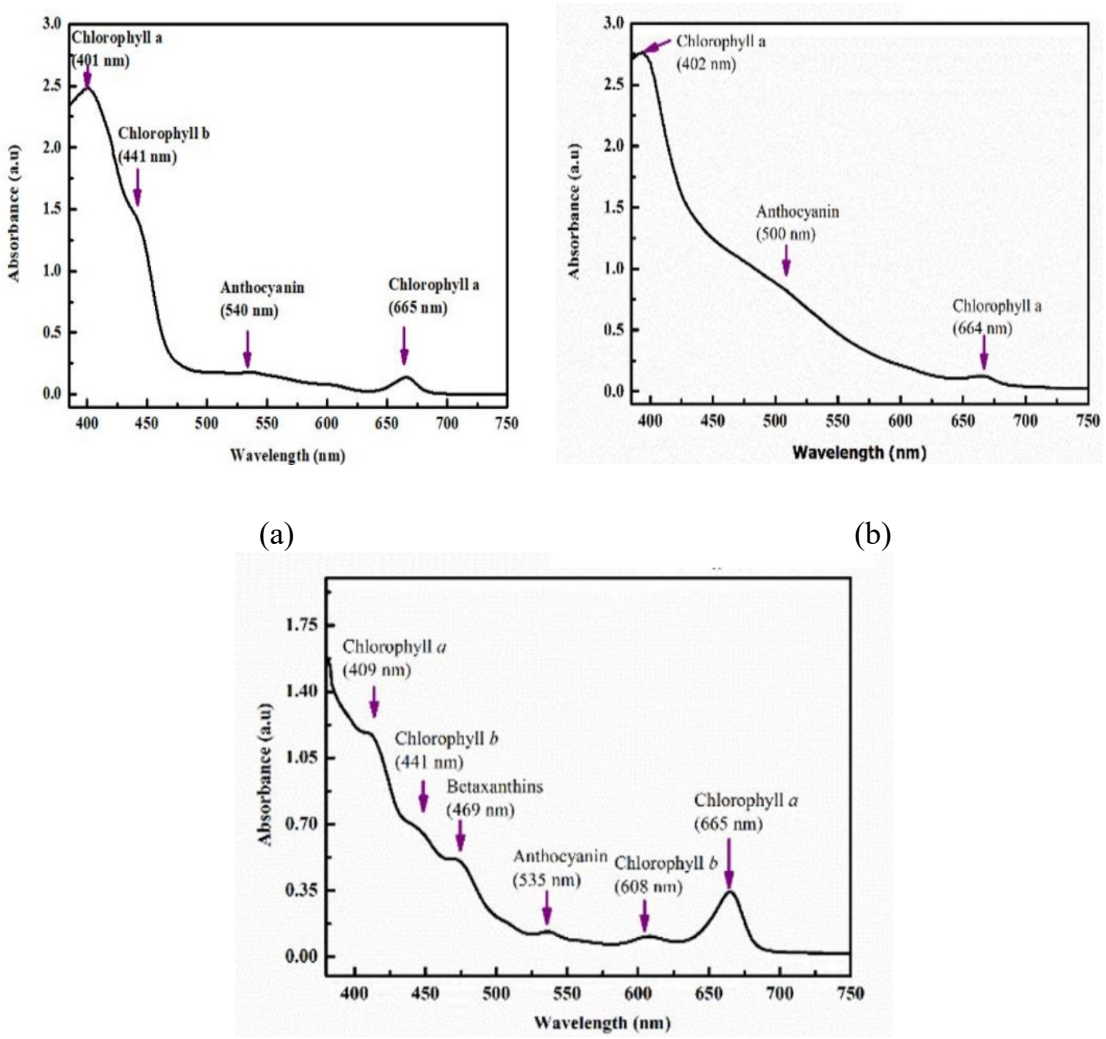

(a) (b)

(c)

Figure 5. UV-vis absorption spectrum of extracted dyes from (a) *Garcinia mangostana l.* pericape, GMP (b) *vitis vinifera* peel, VVP of fruit and (c) violet *bougainvillea sp.* Petal, VBP

Natural dye stability is affected by Light, temperature, pH, anthocyanin structure and pigment. The pH of 100% ethanol is 7.33, whereas the pH of pure water is 7.00. Anthocyanin is one of the sub-classes of phenolic phytochemicals [16]. Anthocyanin exists as a glycoside (anthocyanin glycosides and acrylate anthocyanin). However, anthocyanin is the glycosylated form of anthocyanidins. The conjugated bonds of anthocyanin are present in red, blue and purple−coloured plants [17]. The various UV−Vis absorption is due to the different natural dye sources which consist of other pigments. The GMP and VVP are fruit-based while the VBP is a flower-based dye. Hence the types of anthocyanin molecules may differ [18]. The observed absorption wavelength of the dyes could facilitate the incoming photons and provides necessary excitation energy from the HOMO and LUMO layer [19].

Optical Absorption of GMP, VVP and VBP combined with ZnO nanorod

The dyeing process is applied to ZnO nanorod (ZnOnr) thin films to form coloured nanoporous ZnO photoelectrode. In this research, GMP, VVP and VBP extracts are used to compare the most optimum natural purple dyes that can contribute to the performance of SS-DSSC. Natural Dye VBP thin film absorbs light waves in the range of 200 - 750 nm with low intensity compared to ZnOnr thin film as shown in Figure 6(a). The intensity of light absorption in ZnOnr/VBP increases at 200-400 nm and decreases at 400-750 nm, which means that the ability of ZnOnr/VBP to absorb photon energy in the UV region, is higher than the visible area.

According to Figure 6(a), the total overall performance of an SS-DSSC depends on the dye sensitizer's potential to absorb light and the propagation of the ejected electron through the ZnOnr thin film. The optical absorption spectrum of the ZnOnr exhibited a maximum absorption at 363 nm, whereas the GMP spectrum exhibited three maximum absorptions at 241 nm, 262 nm and 322 nm (UV region 200–400 nm). The optical absorption of ZnOnr/GMP demonstrates that the maximum absorption peak occurs at the same wavelength as ZnOnr and GMP optical absorption, respectively. Mangosteen pericarp dyes and ZnOnr have no chemical bond (π to π^*) because there is no wavelength shift.

The UV−Vis spectrum of the VVP thin film showed two broad peaks at 279 nm and 534 nm are associated to Flavonols(hesperidin) [20] and anthocyanin respectively as shown in Figure 6(b). While ZnOnr/VVP thin film spectra showed a maximum peak at 361 nm associated with ZnOnr, two peaks of flavonols (hesperidin) and anthocyanin did not appear but overlapping absorption. The absorption peak of ZnOnr showed no shifts in ZnOnr/VVP spectra, meaning that no bonding between the dye's chemical groups and the dye's bonding with the ZnOnr surface [15].

The optical absorption spectrum shown in Figure 6(c) explains that VBP thin film absorbs light with low intensity in the 200-750 nm range, as opposed to ZnOnr thin film. However, the absorbance intensity of ZnOnr/VBP increases at 200–400 nm and decreases at 400–750 nm. This means that ZnOnr/VBP can absorb more photon energy in the ultraviolet than in the visible. Optical absorption by pigments found in VBP thin film is weak, with a weak peak recorded at 270 nm which is optical absorption by phenols compound. While, the ZnOnr/VBP spectrum shows a weak peak at 362 nm belonging to ZnOnr and a broad weak peak at 347 nm.

Optical band gap of GMP, VVP and VBP with ZnOnr thin film

The band gap of GMP, VVP and VBP dyes was determined using equations (1) and (2), a direct band gap semiconductor the well-known Tauc relation [21]: hc

$$E_! = \frac{}{|"\#\$} \quad (1)$$

$$(ahu) = C \quad (\quad hu \quad - \quad E_! \quad)^{\%}$$

(2)

The energy gap values of natural dye GMP, VVP and VBP observed in the form of solution and thin film are included in Table 1. The energy gap, E_g for natural dye GMP is 3.20 eV higher than natural dye VVP (2.6 eV) and lower than natural dye VBP (3.34 eV). When the natural dye is combined with ZnOnr, the E_g value for ZnOnr/GMP and ZnOnr/VBP decreases by 7.5 % and 7.7 %, respectively, resulting in 2.98 eV and 2.92 eV, while the E_g of ZnOnr/VVP increases by 12.6 % (2.80 eV).

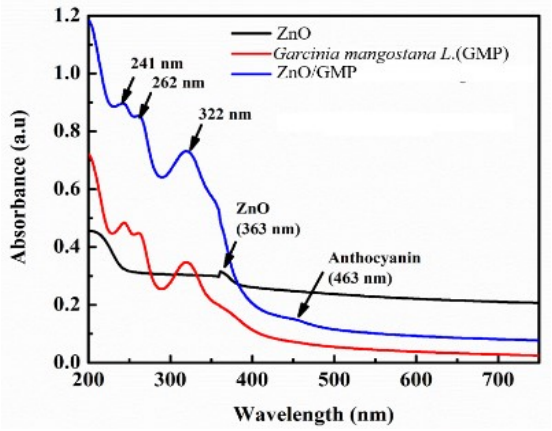

(a)

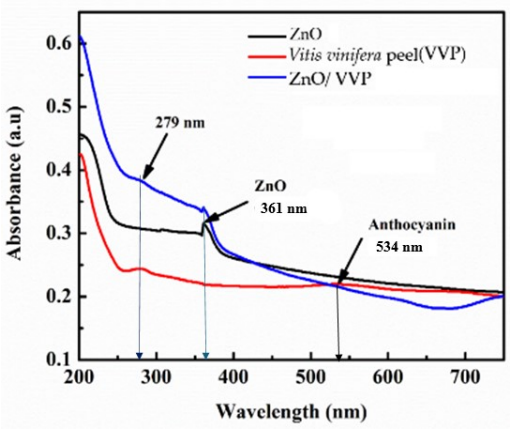

(b)

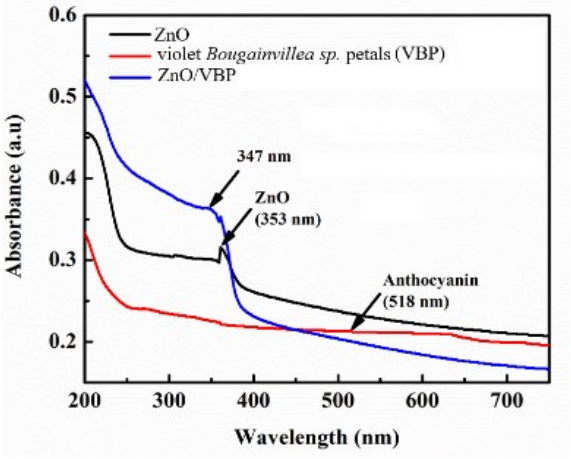

(c)

Figure 6. UV-vis absorption spectrum of ZnOnr/natural Dye thin film from (a) Garcinia mangostana l. pericarp, (b) Vitis vinifera peel of fruit and (c) Violet bougainvillea sp. Petal

Table 1. The energy gap of extracted dyes from GMP, VVP and VBP in ethanol solvent and thin film

Natural Dyes	The energy band gap (eV)	
	In ethanol	Thin film
Garcinia mangostana l. pericarp	1.82	3.22
Vitis Vinifera peel	1.826	2.60
Violet *Bougainvillea sp.*	1.832	3.34
ZnO nanorod (ZnO_{nr})	-	2.65
ZnO_{nr}/GMP	-	2.98
ZnO_{nr}/VVP	-	2.80
ZnO_{nr}/VBP	-	2.92

The performance of SS-DSSC

The performance of the SS-DSSC depends on the dyes, particularly with their visible light absorption criteria. Table 2 provides the result obtained from the performance of the SSDSSC sensitized by GMP, VVP and VBP dyes, respectively. The power conversion efficiency of the SS-DSSC prepared from the extract of GMP was 0.72% with V_{OC} of 6.87 mV, J_{SC} of 0.10 mA/cm^2 and *FF* of 26.7%. The solar cell prepared with VVP extract yielded J_{SC} of 0.04 mA/cm^2, V_{OC} of 6.36 mV, *FF* of 24.8% and conversion efficiency of 0.21%. Hence, the sensitization of dyes shows improvement in SS-DSSC performance because the dyes can harvest light and enhance charge transport in SS-DSSC.

Table 2. Photovoltaic performance of SS-DSSC

Sample	V_{OC} (mV)	J_{SC} (mA/cm^2)	*FF* (%)	η (%)
ITO/ZnO/P3HT/Ag	3.70	1.07	24.9	0.10
ITO/ZnO/GMP/P3HT/Ag	6.87	0.10	26.7	0.72
ITO/ZnO/VVP/P3HT/Ag	6.36	0.04	24.8	0.21
ITO/ZnO/VBP/P3HT/Ag	5.07	0.09	24.8	0.42

The SS-DSSC fabricated using VBPs exhibited a power conversion efficiency of 0.42% with V_{OC} of 5.07 mV, J_{SC} of 0.09 mA/cm^2 and FF of 24.8%. Hence, the sensitization of dyes shows improvement in SS-DSSC performance because the dyes can harvest light and enhance charge transport in SS-DSSC.

The SS-DSSC built of ZnOnr sensitized by GMP dye extract has the highest power conversion efficiency. These results indicate that the different efficiencies are due to the energy transfer mechanism, in which each dye molecule contains different anthocyanin pigments that absorb at a specific wavelength [22]. The higher the anthocyanin values of the dyes, the higher the absorption capacity. Therefore, the SS-DSSC with the sensitizer of GMP is the highest. The mechanism of energy absorption is also applied in the energy conversion process in solar energy [11].

CONCLUSIONS

The conclusion is ZnO nanorods thin films were successfully synthesized by hydrothermal method at 95 °C for 15 min of immersion of ZnO seed in growth solution and showed the average length and diameter of the nanorods are 237 and 76.7 nm, respectively. Then, the ZnO was continued to be applied with natural purple dyes, which are mangosteen pericarp (GMP), black grape peel (VVP) and violet Bougainvillea petal (VBP). Optical absorption of GMP, VVP and VBP in ethanol solvent reveals that anthocyanin pigments are detected at 540 nm, 500 nm and 535 nm, respectively. However, unlike optical absorption in the form of a thin film, the broadened absorption peak appears exclusively in the UV region. When combined with ZnO nanorods, the optical absorption of natural dye increases in the UV region. The energy gap for GMP, VVP and VBP is nearly identical at 1.8 eV; however, when ZnO is added, the Eg value increases to 2.98, 2.80 and 2.92 eV, respectively. The result of power conversion efficiency of SS-DSSC sensitized with GMP produced the highest efficiency at 0.72%. Hence, efforts have now to be made on the conjugated natural purple dyes to further improve the photovoltaic parameters. Future of natural dye research must focus on its stability which involves to combination of natural dye with metal oxide and acid.

ACKNOWLEDGMENTS

The authors thanks to University Malaysia Terengganu with provided the instrument and laboratory. This project was financially supported by the Malaysian Ministry of Higher Education, under the Fundamental Research Grant Scheme (FRGS), FRGS/1/2018/TK10/UMT/02/04 (VOT 59511).

REFERENCES

1. Syafinar R, Gomesh N, Irwanto M, Fareq M, Irwan Y. Potential of purple cabbage, coffee, blueberry and turmeric as nature based dyes for dye sensitized solar cell (DSSC). *Energy Procedia*. 2015;79:799–807.
2. Sofyan AT, Taher M, Monzir S, Hatem G, Amal B, Wael AT. Dyes extracted from safflower, *Medicago sativa* and *Rosmarinus officinalis* as photosensitizers for dyesensitized solar cells. *J Nano Electron Phys*. 2016;8:01026-1–01026-5.
3. Zakiyah A, Mohd Sabri MG, Hasiah S, Azmi Z, Salmah MG, Mohd Azman Z, Emmer Ashraf KM. The conductivity study of hybrid solar cells of TiO_2 and doped with *Bixa orellana* for solar cells application. *J Teknol*. 2015;78:331–5.
4. Ghazali SM, Salleh H, Ghazali MSM, Dagang AN, Zakaria A, Zaini MAMM, Zulkifli MA. Morphological and electrical characterization of hybrid thin-film composed of titania nanocrystals, poly(3-hexylthiophene) and *Piper betle* Linn. *Jurnal Teknologi (Sciences & Engineering)*. 2016;78(3):75–81.
5. Dhafina WA, Daud MZ, Salleh H. The sensitization effect of anthocyanin and chlorophyll dyes on optical and photovoltaic properties of zinc oxide based dyesensitized solar cells. *Optik*. 2020;207:163808.
6. Aziz NN, Isa M, Hasiah S. Electrical and hall effect study of hybrid solar cell. *J Clean Energy Technol*. 2014;2(4):321–5.
7. Nik Aziz N, Isa M, Salleh H. Effect of time conditions on the growth of ZnO nanorods via hydrothermal method. *Adv Mater Res*. 2014;895:509–12.

8. Zakiyah A, Mohd Sabri MG, Hasiah S, Azmi Z, Salmah MG, Mohd Azman Z, Emmer Ashraf KM. The conductivity study of hybrid solar cells of TiO_2 and doped with *Bixa orellana* for solar cells application. *Jurnal Teknologi*. 2015;7:331–5.
9. Ghazali SM, Salleh H, Ghazali MSM, Dagang AN, Zakaria A, Zaini MAMM, Zulkifli MA. Morphological and electrical characterization of hybrid thin-film composed of titania nanocrystals, poly(3-hexylthiophene) and *Piper betle* Linn. *Jurnal Teknologi*. 2016;78(3):75–81.
10. Maadhde TSA, Jumali MH, Al-Agealy HJ, Razak FBA, Yap CC. An investigation of the fill factor and efficiency of molecular semiconductor solar cells. *Mater Sci Forum*. 2021;1039:373-381.
11. De S, Bhattacharya A, Mondal S, Mukhopadhya A, Sen S. Identification and early prediction of lean blowout in premixed flames. *Sādhanā*. 2020;45:1–12.
12. Sajjad M, Ullah I, Khan M, Khan J, Khan MY, Qureshi MT. Structural and optical properties of pure and copper doped zinc oxide nanoparticles. *Results Phys*. 2018;9:1301–9.
13. Balogun SW, James OO, Sanusi YK, Olayinka OH. Green synthesis and characterization of zinc oxide nanoparticles using bashful (*Mimosa pudica*) leaf extract: A precursor for organic electronics applications. *SN Appl Sci*. 2020;2:1468.
14. Yang G, Park S-J. Conventional and microwave hydrothermal synthesis and application of functional materials: A review. *Materials*. 2019;12(7):1177.
15. Shandilya M, Rai R, Singh J. Hydrothermal technology for smart materials. *Adv Appl Ceram*. 2016;115(6):354–76.
16. Pérez MB, Carvajal S, Beretta V, Bannoud F, Fangio MF, Berli F, et al. Characterization of purple carrot germplasm for antioxidant capacity and root concentration of anthocyanins, phenolics, and carotenoids. *Plants*. 2023;12(9):1796.
17. Enaru B, Drețcanu G, Pop TD, Stănilă A, Diaconeasa Z. Anthocyanins: Factors affecting their stability and degradation. *Antioxidants*. 2021;10(12):1967.
18. Gérard V, Ay E, Morlet-Savary F, Graff B, Galopin C, Ogren T, et al. Thermal and photochemical stability of anthocyanins from black carrot, grape juice, and purple sweet potato in model beverages in the presence of ascorbic acid. *J Agric Food Chem*. 2019;67(19):5647–60.
19. Surana K, Bhattacharya B, Majumder S. Extraction of yellow fluorescent *Caesalpinia sappan* L. dye for photovoltaic application. *Opt Mater*. 2021;119:111347.
20. Fauconneau B, Waffo-Teguo P, Huguet F, Barrier L, Decendit A, Merillon J-M. Comparative study of radical scavenger and antioxidant properties of phenolic compounds from *Vitis vinifera* cell cultures using in vitro tests. *Life Sci*. 1997;61(21):2103–10.
21. Rusdi R, Abd Rahman A, Mohamed NS, Kamarudin N, Kamarulzaman N. Preparation and band gap energies of ZnO nanotubes, nanorods and spherical nanostructures. *Powder Technol*. 2011;210(1):18–22.
22. Ezike SC, Hyelnasinyi CN, Salawu MA, Wansah JF, Ossai AN, Agu NN. Synergestic effect of chlorophyll and anthocyanin co-sensitizers in TiO_2-based dye-sensitized solar cells. *Surf Interfaces*. 2021;22:100882.